

# A search for the optical/IR counterpart of the probable Einstein ring source 1830 – 211

S. Djorgovski,<sup>1</sup>\* G. Meylan,<sup>2</sup> A. Klemola,<sup>3</sup> D. J. Thompson,<sup>1</sup> W. N. Weir,<sup>1</sup>  
G. Swarup,<sup>4</sup> A. P. Rao,<sup>4</sup> R. Subrahmanyan<sup>4</sup> and A. Smette<sup>5</sup>

<sup>1</sup>Palomar Observatory, California Institute of Technology, Pasadena, CA 91125, USA

<sup>2</sup>Space Telescope Science Institute, 3700 San Martin Drive, Baltimore, MD 21218, USA

<sup>3</sup>UCO/Lick Observatory, Board of Studies in Astronomy and Astrophysics, University of California, Santa Cruz, CA 95064, USA

<sup>4</sup>Tata Institute of Fundamental Research, Homi Bhabha Road, Bombay 400 005, India

<sup>5</sup>European Southern Observatory, Casilla 567, La Serena, Chile

Accepted 1992 January 29. Received 1992 January 29; in original form 1992 January 14

## SUMMARY

We report the results of deep optical and IR imaging, astrometry, and spectroscopy of the recently identified, probable Einstein ring source 1830 – 211. While no definitive counterpart has been identified, several faint objects have been found in the proximity of the radio positions. The brightest object ( $\sim 20$  mag in the red) is nearly coincident with the north-eastern (NE) component of the radio source; however, it has been identified spectroscopically as a foreground M star. Its presence will make the optical or IR identification of the north-eastern radio component very difficult. The object previously proposed as the possible counterpart by Subrahmanyan *et al.* is probably too far from the radio position to be a viable candidate, as are the other two faint, nearby objects, with typical *R* or *I* magnitudes  $\sim 21$ – $23$ . There is a possible marginal IR detection of an object nearly coincident with the south-western (SW) radio component; its existence needs to be checked by IR imaging in subarcsecond seeing conditions. The follow-up spectroscopy will be extremely difficult, due to the faintness of the possible identifications and the crowding. If previous estimates of the galactic extinction along this line of sight are correct, then 1830 – 211 is optically very faint, and the lensing galaxy is likely to be at a redshift of at least a few tenths.

**Key words:** astrometry – galaxies: active – gravitational lensing – infrared: galaxies – radio continuum: galaxies.

## 1 INTRODUCTION

The remarkable radio morphology of the flat-spectrum source 1830 – 211 (catalogued as PKS 1830 – 210) was discovered by Rao & Subrahmanyan (1988), who proposed that the object represents a gravitationally lensed image. This interpretation was developed further by Swarup *et al.* (1989), Subrahmanyan *et al.* (1990; hereafter SNRS), and Jauncey *et al.* (1991), with more radio data. The interpretation of the source as a strong Einstein ring is now almost certain. Such gravitational lenses are especially interesting, due to their potential as probes of mass distribution in galaxies, measurements of the Hubble constant, etc. (for a review and further references, see Blandford & Narayan 1992). The

high radio flux and the presence of a VLBI core-jet structure are likely to make further studies of this object very fruitful.

However, in order to understand fully and utilize gravitationally lensed images such as this, it is necessary to obtain redshifts of the lensed source and the lensing galaxy, as well as other optical or IR information. With this in mind, we made several attempts to secure an optical identification of this object. The major difficulty is that the source lies in an extremely unfavourable direction for optical studies, at a low Galactic latitude, where the foreground crowding and extinction are heavy, and the exact relation between the optical and radio coordinate systems is sometimes uncertain. It was already obvious from our earliest images that there is no optically bright counterpart, and that the apparent faintness will make the optical and IR follow-up difficult. Here we present our results to date. A preliminary report was presented by Djorgovski *et al.* (1992).

\* Alfred P. Sloan Foundation fellow and Presidential Young Investigator.

## 2 THE DATA AND ASTROMETRY

Initial optical imaging of the field was obtained at the ESO 3.6-m telescope in the *BVR* bands, on the night of UT 1988 May 15, prompted by the first publication by Rao & Subrahmanyan (1988). The seeing was  $\sim 1.5$  arcsec (FWHM), and the effective binned pixel size 0.675 arcsec. Objects which we designate as X and Y were detected close to the radio position. Near-infrared images were obtained at the Palomar 200-inch telescope using the InSb array imager, in the *K* ( $2.2 \mu\text{m}$ ) band, on the night of UT 1989 August 20. The seeing was  $\sim 1.2$  arcsec, and the pixel size 0.313 arcsec. Further optical imaging was obtained at the Palomar 200-inch telescope using the 4-Shooter imager in the Gunn *i* band, on the night of UT 1990 March 21. The seeing was  $\sim 2$  arcsec, and the pixel size 0.334 arcsec. An optical spectrum of object X was also obtained with the 4-Shooter, on the night of UT 1990 March 22, in comparable conditions. Finally, our best optical images so far were obtained at the ESO 3.6-m NTT telescope in the *BR* bands, on the night of UT 1990 March 22. The seeing was  $\sim 0.75$  arcsec, and the pixel size 0.152 arcsec. In all cases, multiple images were obtained, shifted, and co-added. The data were processed using standard techniques. Regrettably, none of the nights was fully photometric, and therefore no exposures of standards were taken. We can make only approximate estimates of the magnitudes, good to about 0.5 mag.

Astrometry of the field was performed in order to obtain the positions of nearby stars and transfer the coordinate system to our CCD and IR images. The lack of stars with known equatorial coordinates within a typical small-field CCD frame called for the separate determination of secondary position reference stars within the frame. This was done independently in three different ways, in order to

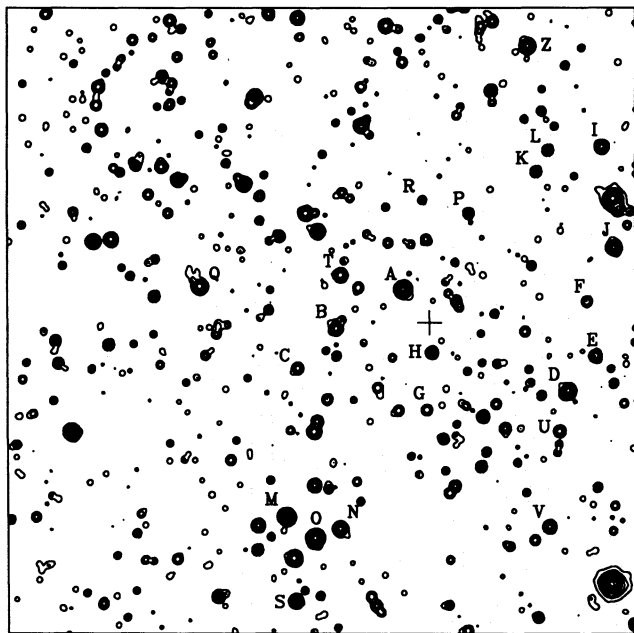


**Figure 1.** Finding chart for the astrometry stars, labelled with letters. This is a section of the *R+I*-band CCD stack frame, obtained at ESO. The field size is 2 arcmin square, with north at the top and east to the left. The mean radio source position is marked with the cross.

control the possible systematics and fully understand the errors. Fig. 1 is a wide-field finding chart of the astrometry stars, with the radio centroid marked with a cross.

First, we used the solution based on stars selected from the Hubble Space Telescope (HST) Guide Star Catalog (the GASP system). The GASP positions are thought to be good to about 0.3–0.7 arcsec. Secondly, we performed the measurements relative to some two dozen nearby SAO stars, using a two-axis measuring engine at the Observatories of Carnegie Institution of Washington, in Pasadena. We compared the positions of SAO stars and Perth 70 southern standards in this general area, and found that there may be systematic shifts between the two systems of the order of 0.1 arcsec in  $\alpha$  and 0.3 arcsec in  $\delta$ . We compared the independent solutions for our field astrometry stars (from GASP and from the measurements using the Carnegie engine), and found that there are systematic shifts between the two solutions of about 0.7 arcsec in  $\alpha$ , and 0.4 arcsec in  $\delta$ . We thus concluded that the *systematic* uncertainties in our coordinate system solutions are of the order of 0.5 arcsec. The random errors from star centring are about 0.2–0.3 arcsec. The net  $1\sigma$  errors are thus  $\sim 0.7$  arcsec, and probably dominated by the systematics. This was the state of affairs when our preliminary report (Djorgovski *et al.* 1992) was prepared. Clearly, a more accurate measurement was needed in a field as crowded as this one.

We therefore performed a third set of measurements, using the recently available Astrographic Catalog of Reference Stars (ACRS) (Corbin & Urban 1989), which we believe to be an improvement over the previously available material. The systematic errors of this catalogue, and the possible systematic differences from the coordinate system assumed in the Very Large Array (VLA) maps, are not yet known. Our rough, subjective estimate based on previous experience is that they may be of the order of  $\sim 0.1$ – $0.2$  arcsec, but we cannot yet offer any firm documentation for this estimate. We used a single wide-field ( $6^\circ \times 6^\circ$ ) plate taken with the yellow lens of the Lick 51-cm double astrograph at epoch 1987.47, originally for the Northern Proper Motion (NPM) programme (Klemola, Jones & Hanson 1987). The plate was measured for precise rectangular coordinates with the recently upgraded version of the Lick Gaertner automatic measuring machine. The measured objects included a set of primary position reference stars taken from the ACRS and a selection of secondary stars distributed over our CCD field. The latter stars are very faint and weak on the deep astrograph plate but constitute the brighter stars on the much deeper CCD frames.

The transformation of the measured rectangular coordinates into equatorial coordinates was made using an astrometric plate reduction model containing the usual linear terms as well as quadratic terms ( $x^2$ ,  $xy$ ) in  $x$  and ( $y^2$ ,  $xy$ ) in  $y$ . The unknown plate constants were evaluated from a least-squares solution using 15 stars from the ACRS as the primary reference frame. This procedure yielded equatorial positions for 14 surviving secondary stars. Of these stars, at least two (L and U) are exceedingly weak and probably should be ignored, while one star (C) is quite weak and possibly of questionable value. It should be noted that still more secondary stars were measured initially within the CCD frame but these did not survive to the final reduction stage, owing to their extreme weakness and image blending.

The derived equatorial coordinates for equinox B1950 are listed in Table 1. Normally the expected random error in equatorial positions derived from a single Lick astrograph yellow plate is about 0.10–0.15 arcsec for better exposed images. In the present application we measured stars towards the plate limit of the astrograph in a very crowded part of the

sky, so that the positional error would be on the higher side. Errors could be still larger (tenths of an arcsecond) for individual secondary stars with undetected blends, or those with very weak images merging with locally non-uniform background grain structure on the film. With 12 (of 14) secondary stars with better positions, such individual random errors should be smoothed out from the CCD frame reductions for the target objects. Those stars successfully measured on the Lick astrograph plate are designated with an asterisk after the star name in Table 1; the coordinates for the other stars are based on subsequent CCD results described next.

We then determined the systematic offsets between the Lick measurements (which we consider to be the most reliable of our three sets) with those from GASP and Carnegie engine measurements. We found differences of  $\Delta\alpha = +0.4$  arcsec and  $\Delta\delta = +0.15$  arcsec in the sense (Lick–GASP), and  $\Delta\alpha = -0.75$  arcsec and  $\Delta\delta = -0.4$  arcsec in the sense (Lick–Carnegie), in agreement with our earlier estimates. Measurements of stars from GASP and the Carnegie engine were brought to the Lick system; the residual rms is in the range  $\sim 0.3$ – $0.6$  arcsec. These coordinates were used for stars where the original Lick measurements were not available.

The final adopted coordinates of the stars are listed in Table 1 (B1950 equinox is used throughout this paper). Finally, from the rms residuals of transformations of equatorial to rectangular coordinates on our frames, and vice versa, we estimate that our random errors are  $\sim 0.3$  arcsec in each coordinate; allowing for combined systematic errors in the ACRS catalogue and Lick plate reductions, assumed by us to be of the order of  $\sim 0.1$  arcsec, the net total  $1\sigma$  errors are estimated to be  $\sim 0.4$  arcsec in each coordinate.

**Table 1.** Positions of field stars.

Star	$\alpha(1950)$	$\delta(1950)$
A*	18 30 40.995	–21 05 54.41
B*	18 30 41.895	–21 06 03.19
C	18 30 42.384	–21 06 11.52
D*	18 30 38.636	–21 06 12.38
E	18 30 38.290	–21 06 04.90
F	18 30 38.431	–21 05 54.70
G	18 30 40.524	–21 06 17.61
H*	18 30 40.514	–21 06 06.21
I*	18 30 38.364	–21 05 24.31
J*	18 30 38.101	–21 05 43.74
K*	18 30 39.190	–21 05 29.59
L	18 30 39.079	–21 05 26.18
M	18 30 42.423	–21 06 39.72
N	18 30 41.681	–21 06 42.05
O	18 30 42.189	–21 06 43.61
P	18 30 40.118	–21 05 39.23
Q*	18 30 43.832	–21 05 56.42
R	18 30 40.751	–21 05 37.78
S*	18 30 42.232	–21 06 56.15
T	18 30 41.832	–21 05 52.69
U	18 30 38.741	–21 06 20.61
V*	18 30 38.794	–21 06 39.75
Z*	18 30 39.491	–21 05 05.57

\*Stars with good Lick positions. Estimated  $1\sigma$  errors are  $\sim 0.4$  arcsec in each coordinate.

### 3 OPTICAL AND INFRARED CANDIDATES

Fig. 2 shows a zoom-in on the radio position on the stack of our ESO *R* and *I* images from 1990 May. The positions of

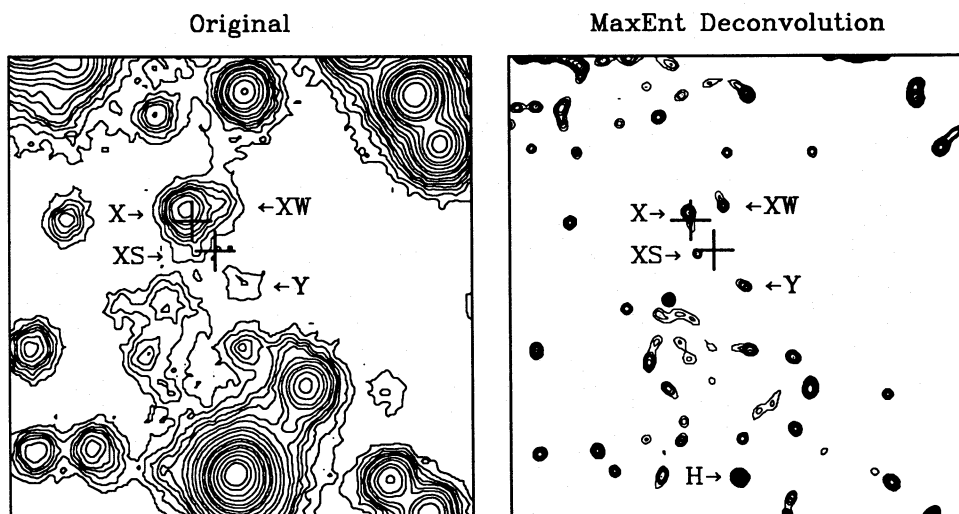


**Figure 2.** A zoom-in on the radio source position on our *R* + *I*-band CCD stack frame. The field size is 12.2 arcsec square, with north at the top and east to the left. The positions of the principal radio source components are marked with crosses, whose sizes correspond to the  $1\sigma$  joint error bars of 0.5 arcsec. Several optical candidates are marked with letters. The bright star just outside the top left-hand corner is star A, and the bright star near the bottom edge centre is star H. The original image is shown on the left, and its seeing deconvolution using a Maximum Entropy (MEM) algorithm on the right. The effective resolution of the MEM-restored image is about 0.2 arcsec.

the two principal components of the radio source (which we will refer to by their relative positions as the NE and SW) are indicated with the  $1\sigma$  crosses. Several objects are visible in the vicinity of the radio positions, and are marked in Fig. 2. Their positions are listed in Table 2, along with the radio source coordinates. The object we denote as Y is the tentative counterpart mentioned by Subrahmanyan *et al.* (1990). Its estimated  $R$  magnitude is about 22 (not 20, as mistakenly stated by Jauncey *et al.* 1991). It is very likely that object Y is actually composed of at least two sources, as it appears elongated roughly in the NE–SW direction. Object X is just barely visible on the ESO/SERC sky survey films, and its  $R$  magnitude is probably close to 20. For objects XW and SE we estimate  $R \sim 21.5$  mag from the relative measurements in our CCD frames, and for object XS,  $R \sim 22.5$  mag. With the exception of the red object X, none of the candidates appears to be particularly blue or red in our data, and we see no evidence for any variability.

Object X is nearly coincident with the NE radio component; object XW is about  $1.5\sigma$  away from it; object XS is about  $1\sigma$  away from the SW component; and object Y is about  $2\sigma$  away from it. We note that the expected optical morphology should be an arcsecond double in the NE–SW direction, possibly with the lensing galaxy between the two components [or closer to the SE component, according to the models by Swarup *et al.* (1989) and Subrahmanyan *et al.* (1990)]. No such combination is readily apparent in our images. The strongest positional coincidence is of course

object X; object Y now does not appear to be a viable candidate.

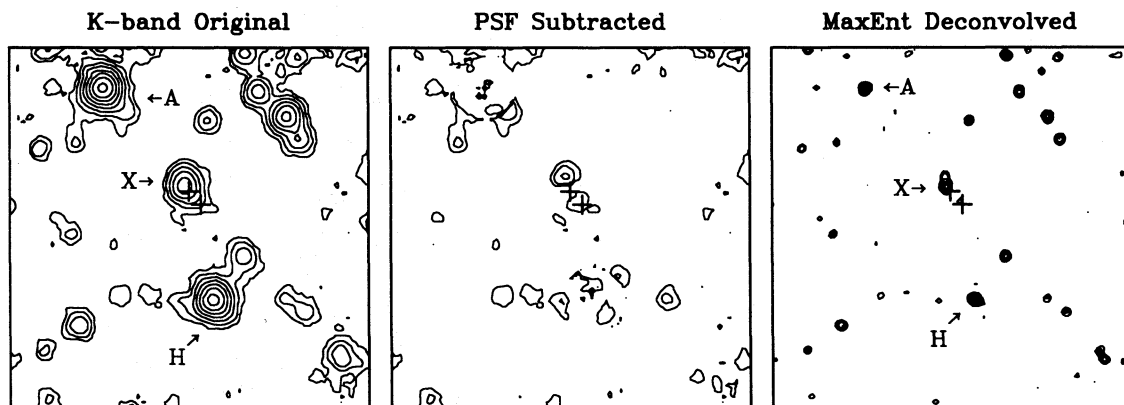
Fig. 2 also shows a restoration of the stack image using a Maximum Entropy algorithm (Weir, in preparation; *cf.* Weir & Djorgovski 1991, and references therein). The seeing deconvolution clearly separates the sources X, XS and XW, and reveals another faint object to the south of X. Object Y has too low a signal-to-noise ratio to be properly resolved by our deconvolution software, and it simply appears elongated.

Fig. 3 shows a  $K$ -band IR image obtained at Palomar. No striking new features are seen in the original image. However, after the point spread function (PSF) subtraction, there are strong residuals near the object X. A Maximum Entropy deconvolution shows a faint companion within 0.5 arcsec north of X, and a possible faint object nearly coincident with the SW radio component. These should be interpreted with some caution: the PSF used is not well determined, due to the smallness of the field and extreme crowding. We would regard the existence of these new IR components only as tentative. We estimate the  $K$  magnitude of object X to be  $\sim 14$ – $15$ ; the new IR components, if real, would have  $K$  magnitudes  $\sim 17$ – $19$ , at the very limit of these data.

Finally, Fig. 4 shows the spectrum of object X; it is clearly a foreground M-type star, probably a main-sequence dwarf. Its rough  $VRK$  colours are consistent with this conclusion. It is thus of no intrinsic interest for identification of 1830 – 211, although it obviously creates a major nuisance, due to its near coincidence with the NE radio component.

**Table 2.** Positions of radio components and optical candidates.

ID	$\alpha$ (1950)	$\pm$	$\delta$ (1950)	$\pm$	Comments
Radio (NE)	18 30 40.643	0.007	–21 05 59.95	0.1	Subrahmanyan <i>et al.</i> (1990)
Radio (SW)	18 30 40.597	0.007	–21 06 00.70	0.1	Ditto
Object X	18 30 40.65	0.029	–21 05 59.7	0.4	Foreground M star
Object XW	18 30 40.58	0.036	–21 05 59.5	0.5	
Object XS	18 30 40.63	0.036	–21 06 01.0	0.5	
Object Y	18 30 40.55	0.036	–21 06 01.6	0.5	Old SNRS candidate



**Figure 3.** An IR image of the field, obtained at Palomar in the  $K$  ( $2.2 \mu\text{m}$ ) band. The field size is 20 arcsec square, with north at the top and east to the left. The positions of the radio source components are marked with crosses, and stars A, H and X are marked with letters. The original stack image is shown on the left, a PSF-subtracted version in the middle, and the seeing-deconvolved Maximum Entropy image on the right. The relative PSF-subtraction residuals from object X are much larger than those for the stars A and H, and are probably real; they may be due to the presence of the IR components also seen in the MEM-deconvolved image, which are *not* seen in the optical data, and may represent the IR counterparts of the lensed object and/or the lens galaxy.



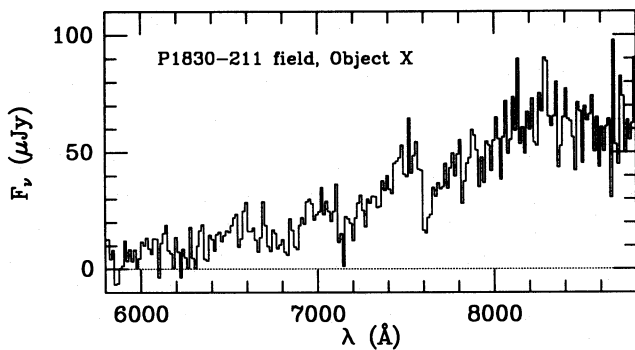


**Figure 4.** A spectrum of the very red object X, obtained at Palomar. It is clearly a foreground M-type star.

#### 4 CONCLUDING REMARKS

We do not have a plausible counterpart of the radio source, down to a red magnitude  $\sim 22$ – $23$ , or  $K$ -band magnitude brighter than about 17. The possible faint IR sources seen in the processed versions of our  $K$ -band images, if real, could represent the counterparts of the radio components and/or the putative lensing galaxy. However, their existence needs to be confirmed by better IR imaging in subarcsecond seeing. At least two examples of extremely red gravitational lenses are now known: MG 1131+0456 (Annis 1992), and MG 0414+0534 (Turner *et al.*, in preparation); 1830–211 may be similar in its optical/IR colours. Unfortunately, the presence of the foreground red star (object X) so close to the NE radio component will make its optical/IR identification extremely difficult.

While the crowding is severe in this direction, the extinction is apparently not very heavy, as few if any very red sources are revealed by the IR images. The estimate of  $A_V \sim 2.7$  mag by Subrahmanyan *et al.* (1990) appears to be quite reasonable. Given our limits on the optical magnitudes of any possible candidates, it is probably safe to conclude that 1830–211 is optically faint (and possibly heavily reddened) and that the lensing galaxy is at a redshift of at least a few tenths.

#### ACKNOWLEDGMENTS

We wish to thank the staff of ESO and Palomar for their help with the observations, Dr Pat McCarthy for help with the Carnegie measuring engine, and Dr Mike Shara and his staff at STScI for the help with the GASP system. Some of the data used here were obtained as a part of the ESO Key Project on Gravitational Lenses, and we wish to acknowledge the efforts of Dr Jean Surdej in heading the Project and securing the observing time. We also thank Dr Wayne Warren, Jr, and staff of the Astronomical Data Center (Goddard Space Flight Center) for the magnetic tape version of the ACRS catalogue. SD acknowledges partial support from the Alfred P. Sloan Foundation, and the US National Science Foundation PYI award AST-9157412. ARK acknowledges the partial support provided by National Science Foundation grant AST-9016521.

#### REFERENCES

- Annis, J., 1992. *Astrophys. J. Lett.*, submitted.  
 Blandford, R. & Narayan, R., 1992. *Ann. Rev. Astr. Astrophys.*, **30**, in press.  
 Corbin, T. E. & Urban, S. E., 1989. In: *Star Catalogues: A Centennial Tribute to A. N. Vyssotsky*, p. 59, ed. Philip, A. G. D., L. Davis Press, Schenectady, NY.  
 Djorgovski, S., Meylan, G., Thompson, D., Weir, N., Swarup, G., Rao, P., Subrahmanyan, R. & Smette, A., 1992. In: *Gravitational Lenses*, eds Kayser, R., Schramm, T. & Refsdal, S., Springer Verlag, Berlin, in press.  
 Jauncey, D. *et al.*, 1991. *Nature*, **352**, 132.  
 Klemola, A. R., Jones, B. F. & Hanson, R. B., 1987. *Astr. J.*, **94**, 501.  
 Rao, P. & Subrahmanyan, R., 1988. *Mon. Not. R. astr. Soc.*, **231**, 229.  
 Subrahmanyan, R., Narasimha, D., Rao, P. & Swarup, G., 1990. *Mon. Not. R. astr. Soc.*, **246**, 263 (SNRS).  
 Swarup, G., Subrahmanyan, R., Narasimha, D. & Rao, P., 1989. In: *Active Galactic Nuclei, IAU Symp. No. 134*, p. 265, eds Osterbrock, D. & Miller, J., Kluwer, Dordrecht.  
 Weir, N. & Djorgovski, S., 1991. In: *Maximum Entropy and Bayesian Methods*, p. 275, eds Grandy, W. & Shick, L., Kluwer, Dordrecht.